JOURNAL OF GEOPHYSICAL RESEARCH, VOL. 114, D21307, doi:10.1029/2009JD012242, 2009

A global comparison of carbon monoxide profiles and column amounts from Tropospheric Emission Spectrometer (TES) and Measurements of Pollution in the Troposphere (MOPITT)

Shu-Peng Ho,[1,2] David P. Edwards,[1] John C. Gille,[1] Ming Luo,[3] Gregory B. Osterman,[3] Susan S. Kulawik,[3] and Helen Worden[1]

Received 13 April 2009; revised 9 July 2009; accepted 21 August 2009; published 6 November 2009.

[1] In this study, we compare carbon monoxide (CO) products from the Measurements of Pollution in the Troposphere (MOPITT) and Tropospheric Emission Spectrometer (TES) and investigate the possible causes of the differences between retrievals for these two data sets. Direct comparisons of CO retrievals for July 2006 show that TES CO concentrations are consistently biased lower than those of MOPITT by 25 ppbv near the surface and by 20 ppbv at 150 hPa, primarily due to different a priori profiles and covariance matrices used in the TES and MOPITT CO retrievals. To reduce the effects of different a priori constraints, we apply TES a priori profiles and covariance matrices to a modified MOPITT retrieval algorithm. The mean TES-MOPITT CO difference decreases from −25 to −10 ppbv near the surface. To further account for retrieval smoothing errors due to different TES and MOPITT averaging kernels, TES averaging kernels are used to smooth MOPITT CO profiles to derive TES-equivalent CO profiles. Compared to these, TES CO profiles are biased 1 ppbv lower near the surface and 4–9 ppbv lower in the troposphere, and the mean absolute TES and TES-equivalent CO column difference is less than 6.5%. The mean TES and MOPITT CO differences due to smoothing errors are close to zero, and the remaining bias is primarily due to the combined effects of radiance biases, forward model errors, and the spatial and temporal mismatches of TES and MOPITT pixels.

Citation: Ho, S.-P., D. P. Edwards, J. C. Gille, M. Luo, G. B. Osterman, S. S. Kulawik, and H. Worden (2009), A global comparison of carbon monoxide profiles and column amounts from Tropospheric Emission Spectrometer (TES) and Measurements of Pollution in the Troposphere (MOPITT), *J. Geophys. Res.*, *114*, D21307, doi:10.1029/2009JD012242.

1. Introduction

[2] Carbon monoxide is one of the few air quality relevant trace gases that can be measured from space. Its sources fall into two main classes: natural chemical production and anthropogenic incomplete combustion processes. In the presence of nitrogen oxides, carbon monoxide (CO) oxidation processes are important in determining the tropospheric ozone (O_3) budget. The principal CO sink is oxidation by the hydroxyl radical resulting in a medium lifetime with a global average of about 2 months. Since this is not long enough for CO to become evenly mixed in the troposphere, it serves as an excellent tracer of transport processes and intense pollution sources that can produce concentration enhancements over background values of several hundred percent [*Edwards et al.*, 2004, 2006]. As a primary indicator of incomplete combustion it can also be used as a proxy for inferring emissions and distributions of other species that are not so readily measured.

[3] Nadir measurements of CO from space using the thermal infrared bands at 4.7 μm are currently being made by instruments on each of the platforms composing the NASA Earth Observing System. In this paper, we present a comparison of CO profile and total column retrievals from the Terra Measurements of Pollution in the Troposphere (MOPITT) and Aura Tropospheric Emission Spectrometer (TES) instruments. Launched in 1999, MOPITT is a multichannel gas correlation radiometer [*Tolton and Drummond*, 1997]. With a total scanning angle of ±26° in each swath and a 22 km × 22 km horizontal resolution, MOPITT is able to generate a global CO map in about 3 days. The equator-crossing time of MOPITT is 1030 LT ± 15 min. The maximum a posteriori (MAP) retrieval method [*Pan et al.*, 1998; *Rodgers*, 2000; *Deeter et al.*, 2003] is used to retrieve CO profile, CO column amount, surface skin temperature, and surface emissivity, and these have been validated by *Deeter et al.* [2003], *Emmons et al.* [2004], *Emmons et al.* [2007], and *Ho et al.* [2002], respectively. The multiyear validation of MOPITT CO vertical profiles and column amounts using a wide range of in situ measurements over ocean and land for different seasons indicates good quan-

[1]National Center for Atmospheric Research, Boulder, Colorado, USA.
[2]COSMIC Project Office, University Corporation for Atmospheric Research, Boulder, Colorado, USA.
[3]Jet Propulsion Laboratory, California Institute of Technology, Pasadena, California, USA.

0148-0227/09/2009JD012242$09.00

titative agreement with the bias mean and standard deviation for the retrieved CO column being $-0.5 \pm 12.1\%$.

[4] Launched in 2004, TES is a high spectral resolution (0.1 cm^{-1} in nadir viewing mode) Fourier transform spectrometer [*Beer et al.*, 2001; *Beer*, 2006]. The equator-crossing time of TES is 1330 LT ± 15 min. With a 5 km × 8 km nadir footprint, it takes around 15 days for TES to generate a global CO map. A Levenberg-Marquardt nonlinear least square method is used to invert TES radiances to CO profiles [*Worden et al.*, 2004; *Bowman et al.*, 2006; *Kulawik et al.*, 2006a]. Although more limited in spatial coverage than MOPITT, the TES measurements have the advantage of additionally providing coincident tropospheric retrievals of other trace gas species (O_3 and some nitrogen compounds), water vapor, and temperature that are also important for studies of tropospheric chemistry. TES CO retrievals have been validated by *Luo et al.* [2007a, 2007b] and *Lopez et al.* [2008].

[5] The objective of this study is to assess the consistency of MOPITT and TES CO data and to investigate the possible causes of differences between these two data sets. Although both MOPITT and TES CO products are retrieved using similar optimal estimation methods [*Rodgers*, 2000], direct comparison is inappropriate. This is because of differences of (1) measurement characteristics (i.e., instrument noise, forward model error, and weighting functions) and (2) predefined retrieval settings (i.e., selection of a priori profiles and background covariance matrices) used by the two algorithms. Moreover, because of different cloud detection techniques employed by the two teams, additional uncertainty may be introduced in the TES and MOPITT CO comparison.

[6] Recently, *Luo et al.* [2007b] showed that 2 days of TES CO retrievals (20–21 September 2004) are consistent with those of MOPITT after accounting for different a priori profile assumptions and vertical resolutions. In their study, an approach introduced by *Rodgers and Connor* [2003] was directly applied to convert MOPITT CO profiles into TES-equivalent CO profiles using TES averaging kernels. However, because TES and MOPITT retrievals are sensitive to CO information at slightly different heights (see section 2.3), information of atmospheric CO variation obtained from MOPITT measurements is effectively smoothed out by this direct conversion.

[7] In this paper, we use a more complete spatial and temporal data comparison than that of *Luo et al.* [2007a] for the month of July 2006. This is also a period after December 2005 when the TES optical bench was set at a warmer operating temperature to improve alignment [*Rinsland et al.*, 2006]. Although multiyear TES and MOPITT data are available, to have an in-depth investigation of the causes of differences through a step-by-step approach (see sections 3 and 4), only 1 month of data is used. We consider three levels of intercomparison of the MOPITT and TES CO products:

[8] 1. Instead of directly applying TES averaging kernels to MOPITT CO to account for the different a priori information in TES and MOPITT retrievals [*Luo et al.*, 2007a], we apply TES CO a priori profiles and covariance matrices to a modified operational MOPITT retrieval algorithm and compare the resulting CO products to TES CO data.

[9] 2. To account for different vertical sensitivities of the TES and MOPITT CO profiles arising from the combined effects of instrument noise, a priori constraint, and measurement weighting functions (see section 2), we use TES averaging kernels to smooth the modified MOPITT CO retrievals from level 1.

[10] 3. To further quantify the effect of the remaining bias differences between TES and modified MOPITT averaging kernels on the CO differences, we sample global CO profiles from the chemical transport Model for Ozone and Related chemical Tracers 3 (MOZART-3) [*Kinnison et al.*, 2007].

[11] In section 2 we describe the TES and MOPITT CO products, retrieval algorithms, and a priori data used in this study. The TES and MOPITT averaging kernels and CO retrievals are also directly compared. This is followed in section 3 by the comparison of TES and MOPITT CO when the TES a priori profiles and covariance matrices are used in MOPITT CO inversion as described in level 1. The TES and MOPITT CO comparisons when TES averaging kernels, a priori, and covariance matrices are applied to MOPITT retrievals (level 2), are presented in section 4. Estimation of CO bias error between TES and MOPITT averaging kernels using MOZART CO profiles (level 3), is also given in section 4. Section 5 concludes this study.

Table 1. Pressure Grids for TES and MOPITT CO Retrievals

Pressure Layer Index for MOPITT	TES Pressure Grid (hPa)	MOPITT Pressure Grid (hPa)
1	1035, 1025, 1010, 1000.0, 908.514	1000
2	825.402, 749.893	850
3	681.291, 618.966, 562.342	700
4	510.898, 464.160, 421.698, 383.117	500
5	348.069, 316.227, 287.298	350
6	261.016, 237.137, 215.444, 195.735, 177.829, 161.561	250
7	146.779, 133.352, 121.152, 110.069, 100.000, 90.8518, 82.5406, 74.9896, 68.1295, 61.8963, 56.2339, 51.0896, 46.4158, 42.1696, 38.3119, 34.8071, 31.6229, 28.7299, 26.1017, 23.7136, 21.5443, 19.5734, 17.7828, 16.1560, 14.6780, 13.3352, 12.1153,11.0070, 10.0000, 9.08514, 8.25402, 6.81291, 5.10898, 4.64160, 3.16227, 2.61016, 2.15443, 1.61560, 1.33352, 1.00000, 0.681292, 0.383118, 0.215443, 0.100000	150

2. TES and MOPITT Retrieval Algorithms

2.1. Retrieval Approach

[12] The TES operational retrieval algorithm follows the optimal estimation approach described by *Rodgers* [1976, 2000]. A Levenberg–Marquardt nonlinear least squares method is used to invert TES radiances to the desired state parameters [*Worden et al.*, 2004; *Bowman et al.*, 2006], which include CO, ozone, and water vapor. TES retrievals are reported in volume mixing ratio (VMR) on a 67 level pressure grid detailed in Table 1. The MOPITT operational retrieval algorithm uses the MAP method [*Pan et al.*, 1998; *Rodgers*, 2000; *Deeter et al.*, 2003], which is also an optimal estimate approach similar to the TES retrieval algorithm. MOPITT CO VMR is reported on a 7 level pressure grid (Table 1).

[13] In the TES retrieval algorithm, the measurement effective cloud contamination is determined from the fre-

quency-dependent optical depths in the 975–1200 cm^{-1} region covered by 25 TES microchannels. The mean cloud optical depth is retrieved together with surface skin temperature, emissivity, and the CO profiles [*Kulawik et al.*, 2006b]. Only TES nadir scenes with mean cloud optical depths less than 0.05 are used here and are considered as clear observations. This approach screens out more than 99% of cloud-contaminated TES pixels. The MOPITT cloud detection uses both MOPITT radiance and a collocated Moderate Resolution Imaging Spectroradiometer (MODIS) cloud mask within the MOPITT field of view to identify the cloudiness of each MOPITT pixel. A cloud flag is provided for each MOPITT pixel (http://www.acd.ucar.edu/mopitt/), and only clear MOPITT pixels are considered here.

[14] In this study, we use MOPITT CO products from a modified version 3 (V3) algorithm for comparison with TES CO data. This is the version described by *Deeter et al.* [2003] with two modifications that are implemented in the newly available MOPITT version 4 (V4) data version. These modifications are (1) a 1° × 1° gridded monthly 4.7 μm surface emissivity (E) [*Ho et al.*, 2005], instead of a globally fixed emissivity, that improves retrievals of surface temperature and CO mixing ratio and (2) retrievals assume a log (VMR) distribution [*Deeter et al.*, 2007a].

2.2. Methodology

[15] The retrieval sensitivity to a CO vertical profile for both TES and MOPITT comes from a broad vertical layer in the troposphere. The retrieved CO profile CO_{MOP} from the MOPITT measurements can be represented as the weighted mean of the true profile (CO_{TRUE}) and the a priori profile (CO_{MOP}^{APR}) [*Rodgers*, 2000]:

$$CO_{MOP} = \mathbf{A}_{MOP} CO_{TRUE} + (\mathbf{I} - \mathbf{A}_{MOP}) CO_{MOP}^{APR}, \quad (1)$$

where $\mathbf{I}$ is the identity matrix and $\mathbf{A}_{MOP}$ is the MOPITT averaging kernel matrix, which represents the sensitivity of the retrieved CO to the true CO, and is given by

$$\mathbf{A}_{MOP} = \frac{\partial CO_{MOP}}{\partial CO_{TRUE}} = \left(K_{MOP}^{T}(\mathbf{S}_{MOP}^{\varepsilon})^{-1}K_{MOP} + (\mathbf{S}_{MOP}^{APR})^{-1}\right)^{-1} K_{MOP}^{T}(\mathbf{S}_{MOP}^{\varepsilon})^{-1}K_{MOP}, \quad (2)$$

where K_{MOP} is the measurement Jacobian or weighting function, $\mathbf{S}_{MOP}^{\varepsilon}$ is the measurement error covariance matrix, and $\mathbf{S}_{MOP}^{APR}$ is the MOPITT retrieval a priori covariance matrix. The retrieval weighting between the a priori assumed state and the real state therefore depends on two a priori constraints: the assumed profile CO_{MOP}^{APR} and the covariance $\mathbf{S}_{MOP}^{APR}$. The CO_{MOP}, CO_{TRUE}, and CO_{MOP}^{APR} in equations (1) and (2) are all vectors. Equation (1) can also be written for the TES CO profile, CO_{TES}, using TES a priori data (CO_{TES}^{APR}) and TES averaging kernels ($\mathbf{A}_{TES}$). The total number of independent pieces of information or the degrees of freedom for signal (DFS) can be obtained by taking the trace of the averaging kernel matrix [*Rodgers*, 2000]. MOPITT and TES are able to provide 1–2 DFS, depending primarily on surface conditions [*Ho et al.*, 2005; *Luo et al.*, 2007a; *Deeter et al.*, 2007a].

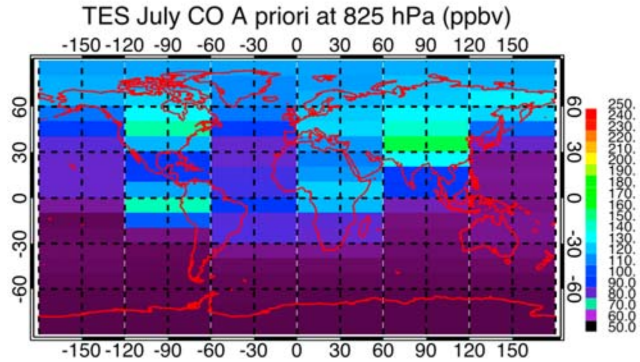

Figure 1. The global TES a priori CO map at 825 hPa for July.

2.3. TES and MOPITT a Priori Description

2.3.1. A Priori Profiles

[16] Monthly mean TES CO a priori profiles are constructed using CO fields from MOZART-3 binned into 60° longitude × 18° latitude regions for each month in 2002. A total of 12 months of a priori CO maps is generated. The global TES a priori CO field at 825 hPa for July is shown in Figure 1. MOPITT V3 uses a global fixed a priori profile, which is constructed from worldwide in situ CO observations [*Deeter et al.*, 2003] (Figure 2).

2.3.2. A Priori Covariance Matrices

[17] The TES a priori covariance matrices (e.g., a priori constraint matrices) are constructed using the Tikhonov method [*Kulawik et al.*, 2006c] for each 36° latitude zone (90°N–54°N, 54°N–18°N, 18°N–18°S, 18°S–54°S, and 54°S–90°S). Current MOPITT V3 algorithm uses a globally fixed a priori profile and background covariance [*Deeter et al.*, 2003] (Figure 2), which is different from that of TES. The vertical distribution of the standard deviations (i.e., the diagonal terms of the covariance matrix) for TES CO a priori covariance matrix for the 54°N–18°N zone is also shown in Figure 2, where a MOZART profile in the 54°N–18°N zone is used as the mean profile. The standard deviation values for TES for other latitudinal zones (not shown) are similar to those at 54°N–18°N. This indicates that the variances of the diagonal terms of the TES covariance matrices are, in general, larger than those of MOPITT at all pressure levels. Except for the tropics (18°N–18°S, not shown), TES variance values are relatively larger between 200 and 500 hPa than those heights below 500 hPa, whereas the largest MOPITT variance values are near the surface and decrease with height. The different a priori constraints used by TES and MOPITT affect the shape and magnitude of their averaging kernels and hence the retrieval results (see sections 2.4 and 2.5).

2.4. Comparison of TES and MOPITT Averaging Kernels

[18] The averaging kernel values depend partly on the assumed retrieval pressure grid since these are intrinsically layer quantities. To see how TES and MOPITT measurements contribute to the retrieved CO profiles differently at each pressure grid, we plot the MOPITT and TES averaging kernels ($\mathbf{A}_{MOP}$ and $\mathbf{A}_{TES}$) at retrieval pressure levels close to those of MOPITT in Figure 3. These representative averag-

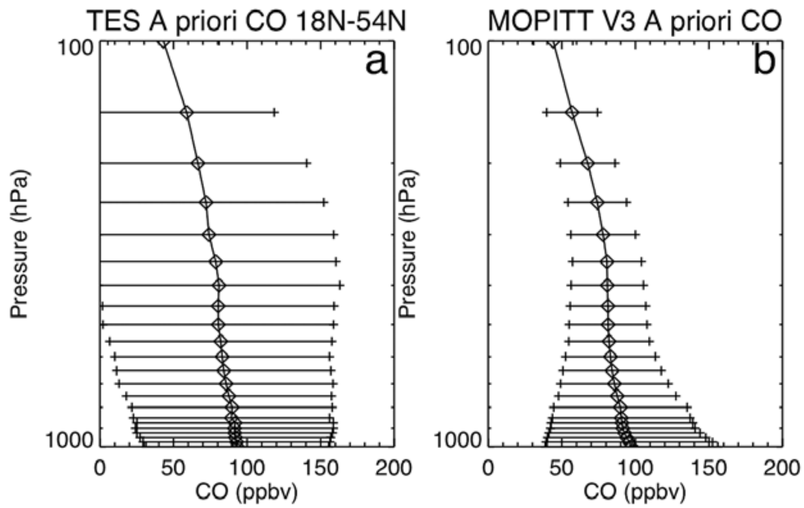

Figure 2. (a) The TES CO a priori profile and its standard deviation, provided by MOZART-3, for the latitude 54°N–18°N zone, and (b) the MOPITT a priori profile and its standard deviation. The TES and MOPITT standard deviations are obtained from the square root of the diagonal terms of TES and MOPITT covariance matrices, respectively. For comparison purposes, the MOPITT covariance matrix is interpolated to a 21 level TES pressure grid between 1000 hPa and 146.8 hPa (see Table 1).

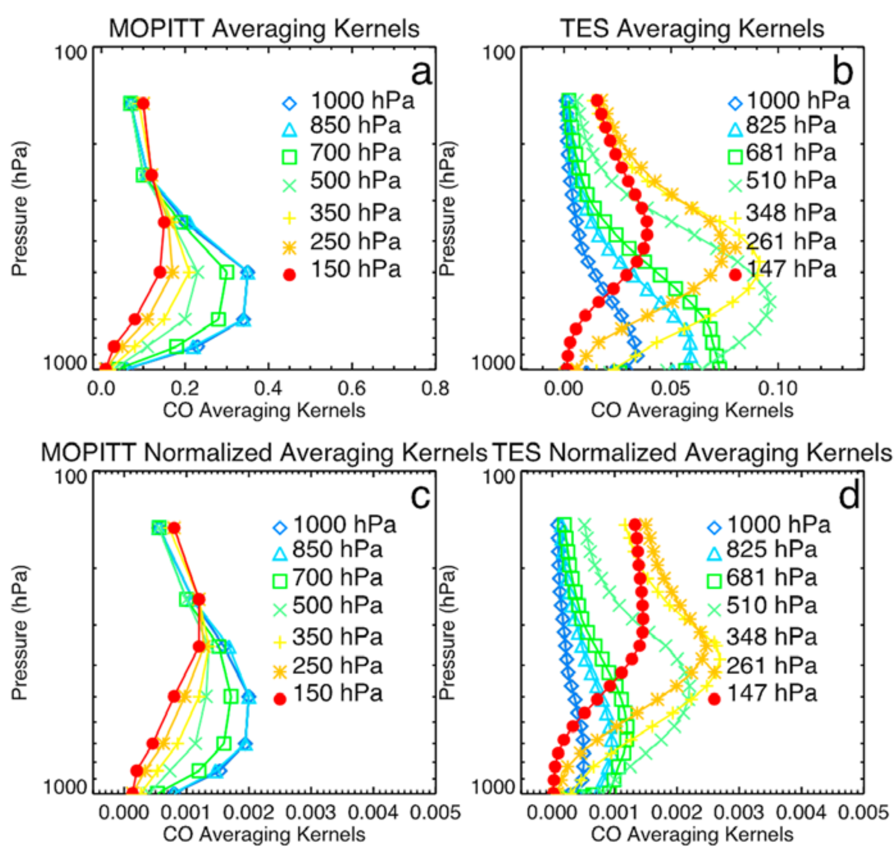

Figure 3. Averaging kernels for 1 July 2006 for (a) MOPITT ($\mathbf{A}_{\mathrm{MOP}}$) at MOPITT pressure levels, (b) TES ($\mathbf{A}_{\mathrm{TES}}$) at the TES pressure levels closest to the MOPITT pressure levels, (c) pressure-layer-normalized averaging kernels for MOPITT ($\mathbf{A}_{\mathrm{MOP}}^{N}$), and (d) pressure-layer-normalized averaging kernels for TES ($\mathbf{A}_{\mathrm{TES}}^{N}$). The unit of the pressure-layer-normalized averaging kernels is hPa^{-1}, and TES averaging kernels are plotted on 21 pressure levels from 1000 to 150 hPa.

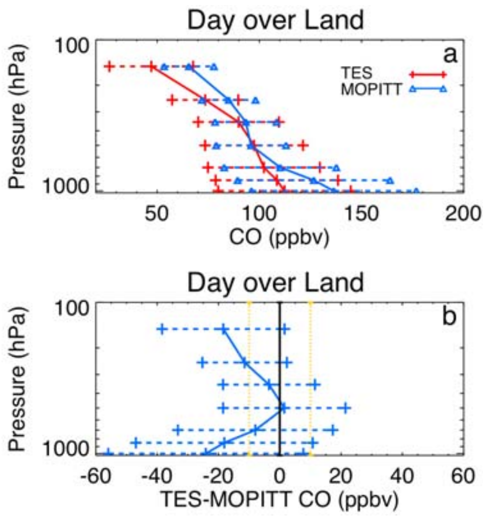

Figure 4. (a) TES and MOPITT global mean profiles (solid red line and blue line, respectively) and standard deviation relative to their means (dashed lines) for July 2006 at MOPITT pressure levels for daytime over land, and (b) the corresponding mean difference between TES CO and MOPITT CO (solid blue line) and their standard deviation (dashed blue line) to the mean. Note that the TES CO retrievals closest to MOPITT pressure levels are used here.

ing kernels, $\mathbf{A}_{\mathrm{MOP}}$ and $\mathbf{A}_{\mathrm{TES}}$, are daytime (both land and ocean) averages from MOPITT and TES on a 1° × 1° collocated grid for 1 July 2006. In general, the shapes of $\mathbf{A}_{\mathrm{MOP}}$ and $\mathbf{A}_{\mathrm{TES}}$ reflect the combined effect of their a priori covariance matrices and weighting functions (not shown) as described in equation (2). The different magnitudes between $\mathbf{A}_{\mathrm{MOP}}$ and $\mathbf{A}_{\mathrm{TES}}$ are mainly due to different pressure layer thicknesses at the retrieval grids used by MOPITT (7 layers) and TES (67 layers), respectively. To make a consistent comparison, we generate the pressure-layer-normalized averaging kernels:

$$\mathbf{A}_{j,k}^{N} = \frac{\mathbf{A}_{j,k}}{\Delta P^{j}}, \qquad (3)$$

where j and k are indexes of column and row elements of $\mathbf{A}$ and $\mathbf{A}^{N}$ and ΔP^{j} is the pressure thickness of the layer corresponding to column index j. After normalization, values of $\mathbf{A}_{\mathrm{MOP}}^{N}$ and $\mathbf{A}_{\mathrm{TES}}^{N}$ for the same rows are now similar in magnitude (Figure 3), where $\mathbf{A}_{\mathrm{TES}}^{N}$ for 147, 348, and 510 hPa peaks mainly above 500 hPa and $\mathbf{A}_{\mathrm{MOP}}^{N}$ for all the levels peaks mainly from 300 to 800 hPa. The different shape and magnitude of the TES and MOPITT averaging kernels combined with their a priori profiles lead to different TES/MOPITT CO retrievals (see section 2.5).

2.5. Comparison of TES and MOPITT CO Retrievals

[19] Because TES is on board the Aura satellite, which is about 3 h behind Terra, it is not possible to find exact coincidence between TES and MOPITT observations. CO has a relatively long chemical lifetime (~2 months global average) and a short time scale variability that depends mainly on transport and source variation. To ensure reasonable coincidence criteria and sample size, we first bin daily MOPITT and TES CO profiles onto a 1° × 1° grid and collocate TES and MOPITT retrievals within 3 h. Because of the difference in instrument sampling, about 25 MOPITT observations (in a 22 km × 22 km horizontal resolution) and one TES observation (in a 5 km × 8 km horizontal resolution) are included in each 1° × 1° grid. More than 3500 1° × 1° gridded TES-MOPITT pairs for July 2006 are used in our comparison.

[20] Figure 4 depicts the TES and MOPITT mean profiles and standard deviation relative to their means and the mean differences between TES and MOPITT CO at MOPITT pressure levels for the July 2006 1° × 1° daily gridded data. TES data at pressure levels closest to MOPITT pressure levels are used in this comparison. The shape and magnitude of TES/MOPITT averaging kernels are strongly affected by the surface thermal contrast conditions [*Ho et al.*, 2005; *Deeter et al.*, 2007b]. Since these are generally largest during the daytime over land, we show comparisons for this (day/land) case. The global mean nighttime averaging kernels (not shown) have a similar shape but a smaller magnitude. It is clear that TES CO concentrations are consistently lower than MOPITT by 25 ppbv near the surface and 20 ppbv at 150 hPa. The smallest differences are found at 500 hPa. The thermal contrast over land at night is generally smaller than during the day, and both TES and MOPITT CO retrievals are weighted more to their respective a priori profiles, especially in the lower troposphere. As a result, the mean MOPITT/TES CO profiles at night over land below 500 hPa (not shown) are about 5–10 ppbv lower than those for day over land.

[21] Figure 5 shows 10° latitudinal mean differences between TES and MOPITT CO at 850, 500, and 250 hPa for the day conditions over both land and ocean. Large TES and MOPITT CO differences at 850 hPa are primarily due to different a priori profiles since at these altitudes the averaging kernels are small. Over cold ocean scenes around 50°S, where thermal contrast is weak, both MOPITT and TES mean CO values at 850 hPa are very close to their respective a priori data. As a result, we have larger TES and MOPITT CO differences. The mean differences and their standard deviations for TES and MOPITT CO profiles for the day for 850, 500, and 250 hPa and the mean absolute difference (MAD) for CO column amount (in %) are summarized in Table 2.

3. Comparison of TES and MOPITT CO Using the Same a Priori Profiles and Matrices

[22] To eliminate the systematic difference of TES and MOPITT comparisons caused by using different a priori profiles and covariance matrices, we apply TES a priori profiles and covariance matrices in the modified MOPITT V3 algorithm. The modified MOPITT CO profile, $\mathrm{CO}_{\mathrm{MOP'}}$, can be written as

$$\mathrm{CO}_{\mathrm{MOP'}} \approx \mathbf{A}_{\mathrm{MOP'}}\mathrm{CO}_{\mathrm{TRUE}} + (\mathbf{I} - \mathbf{A}_{\mathrm{MOP'}})\mathrm{CO}_{\mathrm{TES}}^{\mathrm{APR}}, \qquad (4)$$

where $\mathbf{A}_{\mathrm{MOP'}}$ represents the MOPITT averaging kernels using TES a priori covariance matrices and $\mathrm{CO}_{\mathrm{TES}}^{\mathrm{APR}}$ is the TES CO a priori profile. For comparison with Figure 3c, the

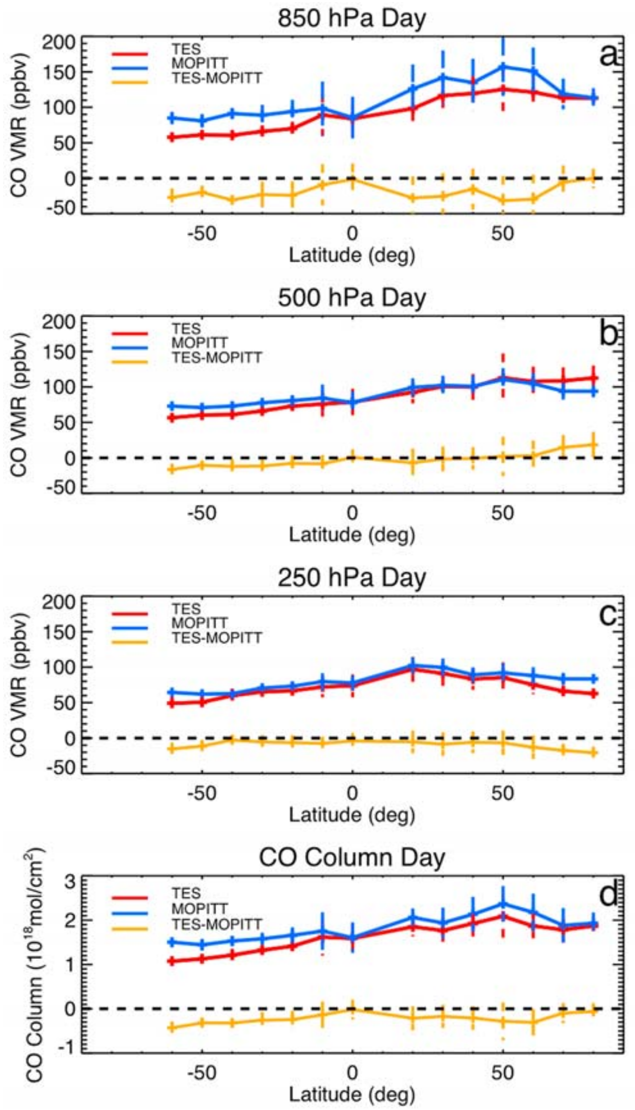

Figure 5. Comparison of 10° latitudinal mean and the standard deviations relative to the mean for TES (red line) and MOPITT CO (blue line) and TES-MOPITT CO (dark yellow line) during daytime at (a) 850 hPa, (b) 500 hPa, (c) 250 hPa, and (d) CO column amount.

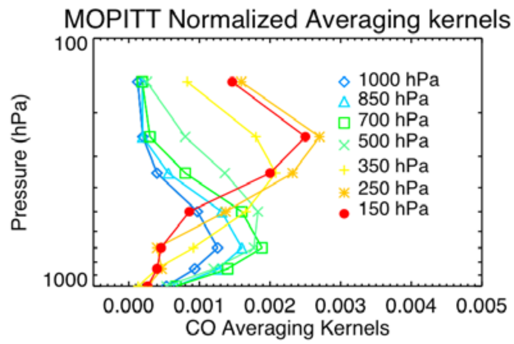

Figure 6. The MOPITT normalized averaging kernels ($\mathbf{A}^N_{MOP'}$) using TES a priori covariance matrices for 1 July 2006. The unit is hPa^{-1}.

normalized MOPITT daytime averaging kernels using TES a priori covariance matrices ($\mathbf{A}^N_{MOP'}$) for 1 July 2006 are plotted in Figure 6. This shows that different constraints affect the shape and magnitude of averaging kernels. Compared to $\mathbf{A}^N_{MOP}$ in Figure 3c, the magnitude of $\mathbf{A}^N_{MOP'}$ for 1000 and 850 hPa decreases about 50% and 30%, respectively. On the other hand, the magnitude of $\mathbf{A}^N_{MOP'}$ at 150, 250, and 350 hPa increases more than 200% compared to those of $\mathbf{A}^N_{MOP}$ at pressure levels between 400 and 200 hPa. Thus, the a priori covariance matrix is responsible for most of this change in shape of averaging kernels because of different diagonal and off-diagonal terms, representing the assumed layer covariance and interlayer correlations, respectively.

[23] Figure 7 compares the global CO statistics for TES (CO_{TES}) and MOPITT using TES a priori (e.g., $CO_{MOP'}$). Mean profiles for July 2006 for day/land are shown. The mean differences between CO_{TES} and $CO_{MOP'}$ are smaller than those in the case of the direct TES and MOPITT CO comparisons in Figure 4. The mean CO difference between MOPITT and TES at 850 hPa decreases from −20 to −10 ppbv for day cases and decreases from −17 to −10 ppbv for night cases (not shown).

[24] With the same a priori profiles and covariance matrices, the zonal mean CO_{TES} and $CO_{MOP'}$ difference at 850 hPa is also smaller than that between CO_{TES} and CO_{MOP} (Figure 8), except in the Southern Hemisphere. The CO_{TES} at 850 hPa in the Northern Hemisphere is only about 10 ppbv lower than $CO_{MOP'}$. The mean difference

Table 2. Comparison Statistics of Mean and Percentage Biases for TES CO and MOPITT CO and the Mean Absolute Total Column Difference for Daytime Over Both Land and Ocean[a]

	$CO_{TES} - CO_{MOP}$	$CO_{TES} - CO_{MOP'}$	$CO_{TES} - CO^{NEW}_{MOP'}$	δCO^{SMOOTH}	δCO^{BIAS}
850 hPa during daytime					
Mean (ppbv)	−12.9 (26.7)	−8.1 (25.4)	−5.3 (14.1)	−1.2 (9.7)	−4.1 (13.3)
Percentage biases (%)	−8.2 (24.7)	−5.7 (24.5)	−4.8 (14.5)	−1.0 (10.4)	−3.7 (14.1)
500 hPa during daytime					
Mean (ppbv)	0.66 (18.2)	−3.9 (19.8)	−5.1 (17.1)	1.4 (11.3)	−6.5 (18.5)
Percentage biases (%)	0.81 (20.2)	−2.5 (22.0)	−5.0 (16.2)	1.5 (15.4)	−6.6 (17.5)
250 hPa during daytime					
Mean (ppbv)	−9.88 (12.7)	−9.7 (15.4)	−9.0 (15.4)	0.2 (6.1)	−9.2 (15.2)
Percentage biases (%)	−11.9 (19.1)	−9.6 (20.0)	−11.0 (17.2)	0.26 (8.3)	−11.2 (17.3)
Mean absolute total column during daytime (%)	7.4 (15.5)	6.94 (15.0)	6.2 (10.7)	0.07 (5.2)	6.4 (10.7)

[a]Comparison statistics are mean and standard deviation of mean. The values of standard deviations are shown in the parentheses. CO_{TES} and CO_{MOP} are TES and MOPITT CO, respectively. $CO_{MOP'}$ is retrieved MOPITT CO using TES a priori and background covariance matrices. $CO^{NEW}_{MOP'}$ is retrieved MOPITT CO using TES a priori and background covariance matrices then smoothed by TES averaging kernels. δCO^{SMOOTH} is the TES − MOPITT CO bias due to smoothing error. δCO^{BIAS} is TES − MOPITT CO bias due to TES/MOPITT radiance biases and forward model errors.

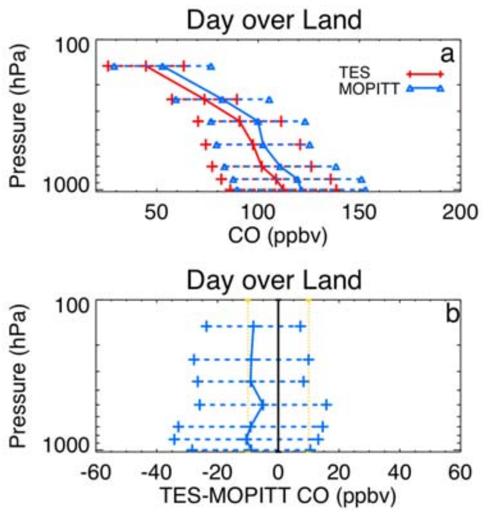

Figure 7. Same as Figure 4 except for CO_{TES} and $CO_{MOP'}$.

($CO_{TES} - CO_{MOP'}$) for the day and its standard deviation at 850, 500, and 250 hPa and the MAD for CO column amount are listed in Table 2. Although the mean CO difference for $CO_{TES} - CO_{MOP'}$ is, in general, smaller than that for $CO_{TES} - CO_{MOP}$, zonal variations of the difference are still large for some regions, especially in the lower troposphere. This is because although we use the same a priori profiles and covariance matrices, relative contributions from the a priori to the retrieved TES and MOPITT CO profile are still different because of remaining differences in the averaging kernels (denoted as smoothing errors hereafter). $\mathbf{A}^{N}_{MOP'}$ for 700, 850, and 1000 hPa in the lower troposphere (Figure 6) is still larger than those of $\mathbf{A}^{N}_{TES}$ in the lower troposphere (Figure 3d) because of the different weighting functions and instrument noise. Possible radiance biases of the TES and MOPITT instruments, forward model error, and temporal and spatial mismatches of TES and MOPITT pixels may also contribute to the remaining difference between CO_{TES} and $CO_{MOP'}$. To make a consistent CO comparison between TES and MOPITT, the effect of the difference in smoothing errors between TES and MOPITT is further reduced in section 4.

4. Comparison of TES CO and MOPITT CO Smoothed by TES Averaging Kernels

4.1. Comparison Methods

[25] To reduce the differences in smoothing errors between MOPITT and TES CO retrievals, we use TES averaging kernels to smooth MOPITT CO profiles as suggested by *Rodgers and Connor* [2003]. The TES-equivalent CO profile converted from $CO_{MOP'}$ (section 3) is defined as

$$CO^{NEW}_{MOP'} \approx \mathbf{A}''_{TES} CO_{MOP'} + (\mathbf{I} - \mathbf{A}''_{TES}) CO^{APR}_{TES}, \qquad (5)$$

where CO^{APR}_{TES} is TES a priori profile and $\mathbf{A}''_{TES}$ is the TES averaging kernel matrix converted to the MOPITT pressure grid using the method introduced by *Deeter et al.* [2007b],

$$\mathbf{A}''_{TES} = \mathbf{A}_{TES}(\Delta P^i / \Delta P^j), \qquad (6)$$

where ΔP^i and ΔP^j are the pressure thicknesses of the layers corresponding to MOPITT retrieval level i and TES retrieval level j, respectively. The averaging kernel matrix for $CO^{NEW}_{MOP'}$ is denoted as $\mathbf{A}^{NEW}_{MOP'}$, that is, equal to $\mathbf{A}''_{TES}\,\mathbf{A}_{MOP'}$.

[26] This method is most applicable to retrieval comparisons where a high vertical resolution measurement is smoothed by the averaging kernels of a much lower resolution measurement [*Rodgers and Connor*, 2003]. In the case of MOPITT and TES the resolutions are comparable. When common a priori constraints are used, application of the combined averaging kernels serves to limit the vertical range of data comparison to that part of the atmosphere where the weighting functions of both measurements are significant. As used here, the technique may be useful for isolating differences in a measurement comparison, but it should not be considered for wider science applications since it essentially serves to smooth away measurement information. Because the vertical resolution

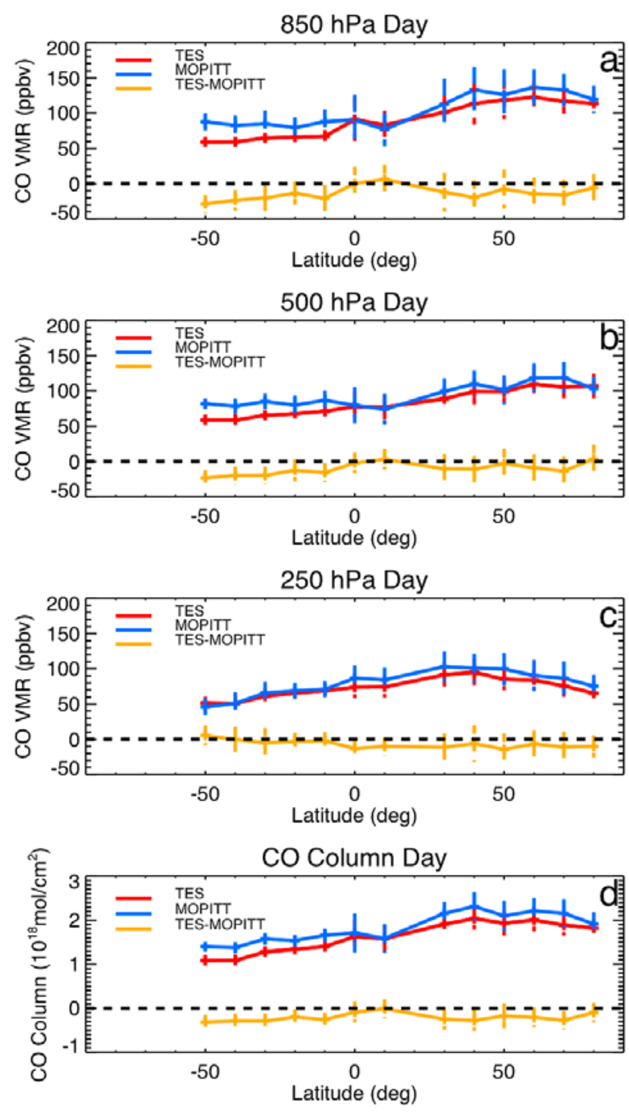

Figure 8. Same as Figure 5 except for CO_{TES}, $CO_{MOP'}$, and $CO_{TES} - CO_{MOP'}$ and their corresponding total column amount.

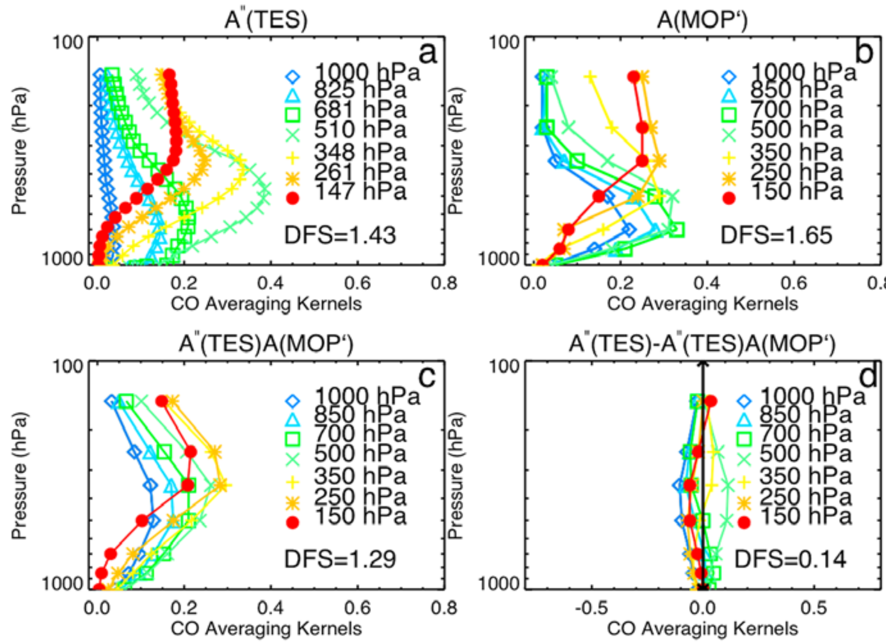

Figure 9. Averaging kernels for daytime for 1 July 2006. (a) TES averaging kernels converted to the MOPITT pressure levels, $\mathbf{A}''_{\mathrm{TES}}$, (b) MOPITT averaging kernels using TES a priori covariance matrices, $\mathbf{A}_{\mathrm{MOP}'}$, (c) $\mathbf{A}_{\mathrm{MOP}'}$ resmoothed by $\mathbf{A}''_{\mathrm{TES}}$ (i.e., $\mathbf{A}''_{\mathrm{TES}}\mathbf{A}_{\mathrm{MOP}'}$), and (d) $\mathbf{A}''_{\mathrm{TES}} - \mathbf{A}''_{\mathrm{TES}}\mathbf{A}_{\mathrm{MOP}'}$.

of $\mathbf{A}''_{\mathrm{TES}}$ is comparable to, yet usually smaller than, that of MOPITT (examples can be see in section 4.2), in equation (5) we use $\mathbf{A}''_{\mathrm{TES}}$ to smooth MOPITT CO retrievals.

[27] The difference between TES and the new MOPITT CO (e.g., $\mathrm{CO_{TES}} - \mathrm{CO}^{\mathrm{NEW}}_{\mathrm{MOP}'}$) can be separated into (1) the CO bias due to smoothing error, $\delta\mathrm{CO}^{\mathrm{SMOOTH}}$, owing to differences between TES and the double-smoothed MOPITT averaging kernels and (2) TES and MOPITT CO biases, $\delta\mathrm{CO}^{\mathrm{BIAS}}$, due to TES/MOPITT radiance biases and forward model errors (denoted as $\Sigma\varepsilon$). According to *Rodgers and Connor* [2003], these two terms can be estimated using the following equation (e.g., equation (29) from *Rodgers and Connor* [2003], which can also be derived from equations (1) and (5)):

$$\mathrm{CO_{TES}} - \mathrm{CO}^{\mathrm{NEW}}_{\mathrm{MOP}'} = \underbrace{\left(\mathbf{A}''_{\mathrm{TES}} - \mathbf{A}''_{\mathrm{TES}}\mathbf{A}_{\mathrm{MOP}'}\right)\left(\mathrm{CO_{True}} - \mathrm{CO}^{\mathrm{APR}}_{\mathrm{TES}}\right)} + \underbrace{\Sigma\varepsilon}$$
$$= \delta\mathrm{CO}^{\mathrm{SMOOTH}} + \delta\mathrm{CO}^{\mathrm{BIAS}}. \qquad (7)$$

4.2. Comparison of TES and Smoothed MOPITT Averaging Kernels

[28] For the comparison technique described in section 4.1 to be valid, the TES averaging kernels and the smoothed MOPITT averaging kernels should have a similar shape and magnitude and have roughly the same DFS. To examine the difference between TES and smoothed MOPITT averaging kernels, we compare $\mathbf{A}^{\mathrm{NEW}}_{\mathrm{MOP}'}$, $\mathbf{A}''_{\mathrm{TES}}$, $\mathbf{A}_{\mathrm{MOP}'}$, and $\mathbf{A}''_{\mathrm{TES}} - \mathbf{A}^{\mathrm{NEW}}_{\mathrm{MOP}'}$ for daytime on 1 July 2006 in Figure 9. It shows that $\mathbf{A}''_{\mathrm{TES}}$ is similar in shape to $\mathbf{A}^{N}_{\mathrm{TES}}$ (Figure 3d) but has a similar magnitude to $\mathbf{A}_{\mathrm{MOP}}$ (Figure 3a). The vertical resolution of $\mathbf{A}^{\mathrm{NEW}}_{\mathrm{MOP}'}$ is strongly related to the relative magnitude and shape of $\mathbf{A}''_{\mathrm{TES}}$ and $\mathbf{A}_{\mathrm{MOP}'}$. With a different profile vertical sensitivity from MOPITT, $\mathbf{A}''_{\mathrm{TES}}$ smoothes out large $\mathbf{A}_{\mathrm{MOP}'}$ values below 500 hPa but preserves large $\mathbf{A}_{\mathrm{MOP}'}$ values above 500 hPa. DFS for $\mathbf{A}''_{\mathrm{TES}}$ and $\mathbf{A}_{\mathrm{MOP}'}$ is equal to 1.43 and 1.65, respectively. The DFS for $\mathbf{A}^{\mathrm{NEW}}_{\mathrm{MOP}'}$ ($= \mathbf{A}''_{\mathrm{TES}}\mathbf{A}_{\mathrm{MOP}'}$) is equal to 1.29. Now $\mathbf{A}^{\mathrm{NEW}}_{\mathrm{MOP}'}$ is more consistent with $\mathbf{A}''_{\mathrm{TES}}$ than $\mathbf{A}_{\mathrm{MOP}'}$ is with $\mathbf{A}''_{\mathrm{TES}}$, where both $\mathbf{A}^{\mathrm{NEW}}_{\mathrm{MOP}'}$ and $\mathbf{A}''_{\mathrm{TES}}$ for all levels are larger above 500 hPa but smaller below 500 hPa. The DFS for $\mathbf{A}''_{\mathrm{TES}} - \mathbf{A}^{\mathrm{NEW}}_{\mathrm{MOP}'}$ is equal to 0.14, which indicates that $\mathrm{CO}^{\mathrm{NEW}}_{\mathrm{MOP}'}$ is able to reasonably present around 90% information content for $\mathrm{CO_{TES}}$.

[29] Note that if common a priori constraints are not used in this method, i.e., $\mathbf{A}_{\mathrm{MOP}}$ is used directly in equation (4) replacing $\mathbf{A}_{\mathrm{MOP}'}$ with $\mathbf{A}_{\mathrm{MOP}}$, then because the shape and magnitude of $\mathbf{A}_{\mathrm{MOP}}$ are very different from those of TES ($\mathbf{A}''_{\mathrm{TES}}$), the shape and magnitude of the combined averaging kernel ($\mathbf{A}''_{\mathrm{TES}}\mathbf{A}_{\mathrm{MOP}}$) are very different from those of $\mathbf{A}''_{\mathrm{TES}}$. As a result, the oversmoothed MOPITT CO profile contains very little CO information and is very close to the MOPITT a priori profiles as demonstrated by *Luo et al.* [2007a].

4.3. Comparison of TES and Smoothed MOPITT CO Retrievals

[30] Figure 10 compares global statistics for $\mathrm{CO_{TES}}$ and $\mathrm{CO}^{\mathrm{NEW}}_{\mathrm{MOP}'}$. Shown are the mean $\mathrm{CO_{TES}}$, $\mathrm{CO}^{\mathrm{NEW}}_{\mathrm{MOP}'}$, and $\mathrm{CO_{TES}} - \mathrm{CO}^{\mathrm{NEW}}_{\mathrm{MOP}'}$ for each MOPITT pressure level for July 2006 for the day/land case. In general, the mean differences between $\mathrm{CO_{TES}}$ and $\mathrm{CO}^{\mathrm{NEW}}_{\mathrm{MOP}'}$ at all vertical levels for day/land (also for daytime over ocean (day/ocean), nighttime over land (night/land), and nighttime over ocean (night/ocean), not shown) are smaller than those between $\mathrm{CO_{TES}}$ and $\mathrm{CO_{MOP'}}$ in Figure 7, especially for those below 500 hPa. Since both $\mathrm{CO_{TES}}$ and $\mathrm{CO}^{\mathrm{NEW}}_{\mathrm{MOP}'}$ are strongly constrained by the TES a priori profiles below 500 hPa, the mean bias decreases from -10 ppbv for $\mathrm{CO_{TES}} - \mathrm{CO_{MOP'}}$ to -1 ppbv near the surface. After minimizing the difference in smoothing errors between the TES and MOPITT averaging kernels,

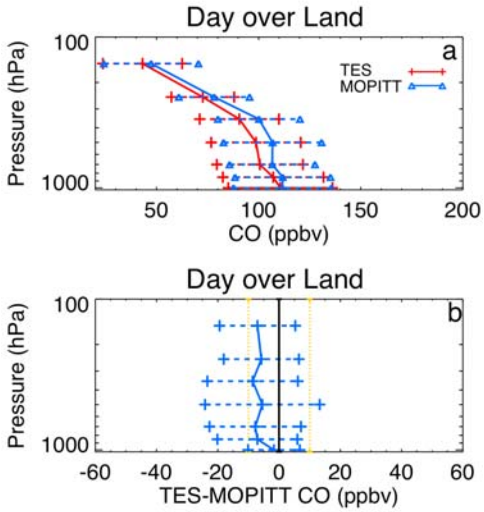

Figure 10. Same as Figure 4 except for CO_{TES} and $CO^{NEW}_{MOP'}$.

the standard deviation relative to the mean differences between CO_{TES} and $CO^{NEW}_{MOP'}$ dramatically decreases when compared to that of the mean of $CO_{TES} - CO_{MOP'}$. Compared to the standard deviation of the mean of $CO_{TES} - CO_{MOP'}$ in Figure 7, the standard deviation of the mean $CO_{TES} - CO^{NEW}_{MOP'}$ decreases by more than 35% below 500 hPa. Above 500 hPa, the difference between CO_{TES} and $CO^{NEW}_{MOP'}$ is still very small. Correlation coefficients for the CO_{TES} and $CO^{NEW}_{MOP'}$ ensemble at MOPITT pressure grids (from surface to 150 hPa) are 0.95, 0.87, 0.85, 0.8, 0.76, 0.86, and 0.86, which are about 20% higher than those between CO_{TES} and $CO_{MOP'}$ and 40% higher than those between CO_{TES} and CO_{MOP} (not shown). The correlation coefficient of column amounts for CO_{TES} and CO^{NEW}_{MOP} is 0.91. This indicates that application of equation (5) reduces the TES and MOPITT CO bias and its standard deviations especially in the lower troposphere that were due to the difference of TES and MOPITT averaging kernels.

[31] Figure 11 shows the 10° mean latitudinal variation of CO_{TES} and $CO^{NEW}_{MOP'}$ at 850, 500, and 250 hPa for day over both land and ocean. In the lower troposphere, CO_{TES} is lower than $CO^{NEW}_{MOP'}$ by less than 4.8% (1–4 ppbv). CO_{TES} is lower than $CO^{NEW}_{MOP'}$ by 5% (1–8 ppbv) in the midtroposphere (500 hPa), whereas the bias is about 2–10% lower in the upper troposphere (2–9 ppbv; Table 2).

4.4. CO Bias due to Differences in Smoothing Error

[32] Although $\mathbf{A}''_{TES} - \mathbf{A}^{NEW}_{MOP'}$ (Figure 9d) is small, to quantify the possible CO bias due to remaining difference between $\mathbf{A}''_{TES}$ and $\mathbf{A}^{NEW}_{MOP'}$, we examine the CO bias due to smoothing error between CO_{TES} and $CO^{NEW}_{MOP'}$, that is, δCO^{SMOOTH} in equation (7). Since we do not know the true CO profile, this is represented here by 2.8° × 2.8° gridded output from the MOZART-3 model (details at http://gctm.acd.ucar.edu/mozart/index.shtml). Inventories such as Emission Database for Global Atmospheric Research (EDGAR) [*Olivier et al.*, 1999] are used to generate the free run MOZART CO profiles, CO_{MOZ}. CO_{MOZ} is within 5 ppbv compared to MOPITT CO profiles in midlatitudes and tropical regions and may have larger difference at high latitudes (NCAR MOZART Team, personal communication, 2008). The closest CO_{MOZ} to the collocated TES and MOPITT CO profile is used.

[33] Figure 12 depicts mean δCO^{SMOOTH} profiles and standard deviation for July 2006 for day/land. In general, δCO^{SMOOTH} is less than 3 ppbv at all pressure levels for day/land and also for day/ocean, night/land, and night/ocean (not shown). The standard deviations of δCO^{SMOOTH} at all levels for day/land are within 12 ppbv. For day/land, δCO^{SMOOTH} ranges from −1.2 to 1.4 ppbv from 850 to 500 hPa (Figure 12).

[34] The mean δCO^{SMOOTH} in each 10° latitude bin is very close to zero (not shown). Their mean difference and its standard deviation for day over both land and ocean at 850, 500, and 250 hPa and the MAD for CO column amount (in %) are listed in Table 2. Note that because TES and MOPITT averaging kernels in equation (7) are actually from TES and MOPITT retrievals within 3 h,

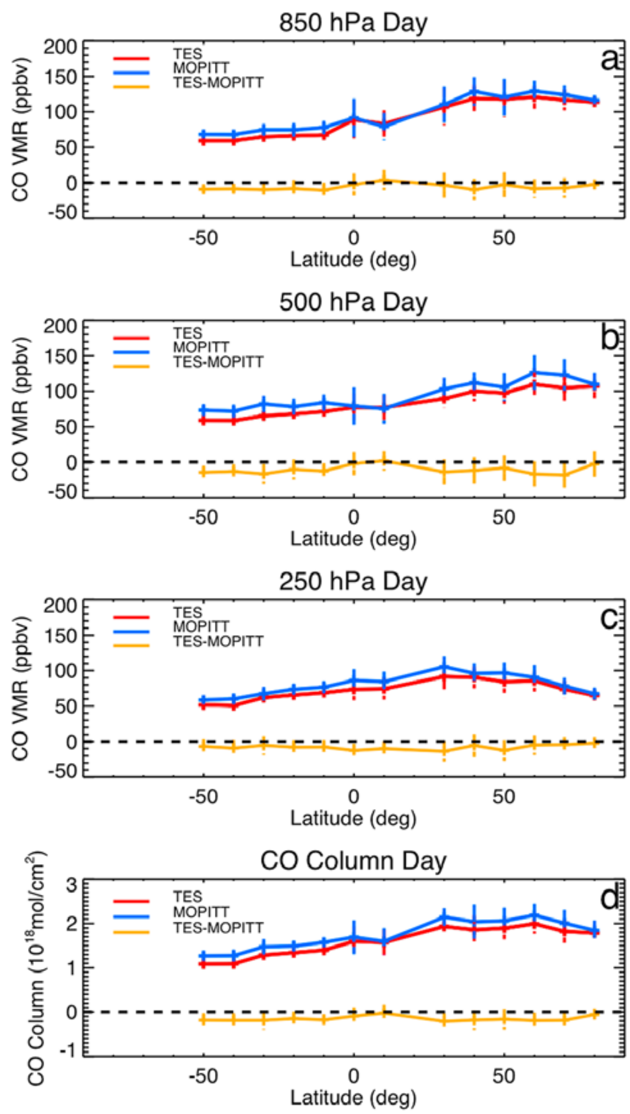

Figure 11. Same as Figure 5 except for CO_{TES}, $CO^{NEW}_{MOP'}$, and $CO_{TES} - CO^{NEW}_{MOP'}$ and their corresponding total column amount.

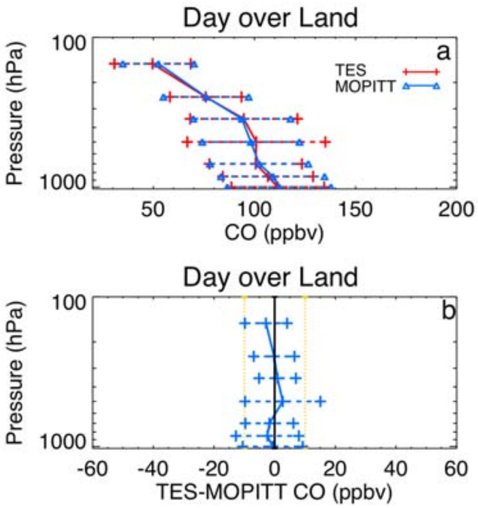

Figure 12. (a) The global mean profiles and standard deviation relative to their means for MOZART-simulated TES CO ($CO_{TES}^{SMOOTH} = \mathbf{A}''_{TES}(CO_{MOZ} - CO_{TES}^{APR}) + CO_{TES}^{APR}$) and MOPITT CO ($CO_{MOP'}^{SMOOTH} = \mathbf{A}''_{TES}\mathbf{A}_{MOP'}(CO_{MOZ} - CO_{TES}^{APR}) + CO_{TES}^{APR}$) for July 2006 at MOPITT pressure levels during daytime and (b) the corresponding mean difference between CO_{TES}^{SMOOTH} and $CO_{MOP'}^{SMOOTH}$ ($\delta CO^{SMOOTH} = CO_{TES}^{SMOOTH} - CO_{MOP'}^{SMOOTH}$) and their standard deviation relative to the mean difference.

possible CO differences due to thermal contrast variations for TES and MOPITT pixels within 3 h have already been included in the analysis.

4.5. Remaining CO Bias

[35] After eliminating the smoothing error, the remaining difference between TES and MOPITT CO can be attributed to the combined effects of radiance bias, spatial and temporal mismatches of TES and MOPITT pixels, and possible forward model errors. Figure 13 compares the global statistics for TES and the new MOPITT CO with the corresponding smoothing errors subtracted, δCO^{BIAS} (= $CO_{TES} - CO_{MOP'}^{NEW} - \delta CO^{SMOOTH}$), for each MOPITT pressure level for the July 2006 day/land case. Because the estimated smoothing error is very close to zero, the remaining CO bias, δCO^{BIAS}, is very close to that of $CO_{TES} - CO_{MOP'}^{NEW}$ in Figure 10. The mean TES-retrieved CO is consistently lower, though only by a small amount, than that of MOPITT. The 10° mean latitudinal variation of δCO^{BIAS} is very close to that of $CO_{TES} - CO_{MOP'}^{NEW}$ in Figure 11 (not shown).

[36] The mean difference and standard deviation from the mean difference for δCO^{BIAS} profiles for day over both land and ocean for 850, 500, and 250 hPa and the MAD for CO column amount are summarized in Table 2. The mean bias is within 4–11% at all levels. The mean absolute TES and MOPITT CO column difference is less than 6.5%.

5. Conclusions and Future Work

[37] In this study, we investigate the possible causes of the differences between the retrievals of the MOPITT and TES CO products. Different from *Luo et al.* [2007a], here we applied the TES a priori to a modified operational MOPITT retrieval algorithm to account for the different a priori information in TES and MOPITT retrievals. The resulting MOPITT CO in July 2006 was compared to TES CO in the same month. We reached the following conclusions:

[38] 1. Compare TES and MOPITT CO retrievals. Direct comparisons of CO retrievals for July 2006 show that TES CO concentrations are consistently biased lower than those of MOPITT by 25 ppbv near the surface and by 20 ppbv at 150 hPa, primarily due to different a priori profiles and covariance matrices used in the TES and MOPITT CO retrievals. The predefined vertical pressure grids used by MOPITT and TES also strongly affect the shape and magnitude of their corresponding averaging kernels and lead to TES and MOPITT CO differences. The pressure-layer-normalized averaging kernels for MOPITT and TES actually peak at different heights. TES pressure-layer-normalized averaging kernels for 348, 261, and 147 hPa peaks above 500 hPa, where MOPITT pressure-layer-normalized averaging kernels for all levels, except at 150 hPa, peaks between 300 and 800 hPa.

[39] 2. Compare TES and MOPITT CO using the same a priori profiles and matrices. When a modified MOPITT retrieval uses the same a priori profiles and covariance matrices as TES, the mean difference between the TES and modified MOPITT CO decreases to −10 ppbv near the surface. The mean difference between TES and MOPITT CO is within 10 ppbv at all vertical levels where the standard deviations to its mean are still large because of the remaining difference in the averaging kernels (i.e., smoothing errors).

[40] 3. Reduce the smoothing error between TES and MOPITT CO. To reduce the smoothing error between TES and MOPITT CO, TES averaging kernels are used to smooth MOPITT CO profiles. The mean CO bias between

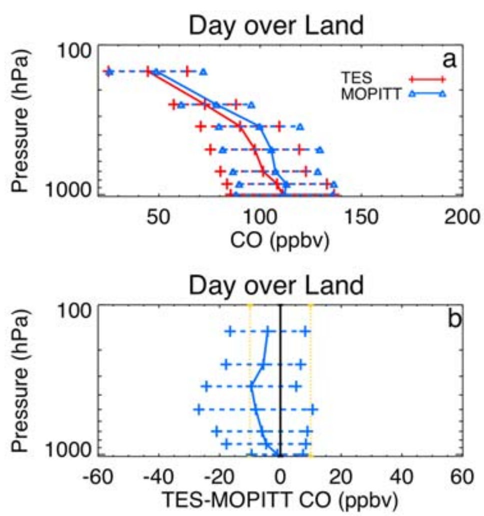

Figure 13. (a) The global mean profiles and standard deviation relative to their means for TES CO and the new MOPITT CO with the corresponding smoothing errors subtracted (red and blue lines, respectively) for July 2006 at MOPITT pressure grids during the daytimes over land and (b) the remaining TES and MOPITT CO mean bias ($\delta CO^{BIAS} = CO_{TES} - CO_{MOP'}^{NEW} - \delta CO^{SMOOTH}$) and the standard deviation relative to the mean bias.

TES and MOPITT is as small as 1 ppbv near the surface and 4–9 ppbv at levels above surface. The MAD of CO column between TES and MOPITT is less than 6.5%. The mean standard deviation to its mean between TES and MOPITT CO is within 20% for all levels which is a decrease of about 35% in comparison to the case of not accounting for the difference of the TES and MOPITT averaging kernels.

[41] 4. Estimate CO bias due to differences in smoothing error (δCO^{SMOOTH}). Global CO from MOZART-3 has been used to estimate δCO^{SMOOTH}. We find that mean δCO^{SMOOTH} at different heights for all latitudes are very close to zero. Over land, δCO^{SMOOTH} ranges from -1.2 to 1.4 ppbv from 850 to 500 hPa. The mean δCO^{SMOOTH} in each 10° latitudinal bin is very close to zero. After removing the effect of δCO^{SMOOTH}, TES CO is consistently smaller than that from MOPITT. The mean bias is within 4–11% at all levels. The MAD of TES and MOPITT CO column is less than 6.5%. The remaining bias is primarily due to the combined effects of radiance biases, forward model errors, and the spatial and temporal mismatches of TES and MOPITT pixels.

[42] The results presented here demonstrate that to have a valid comparison between similar data products, it is essential to account for not only the differences of their a priori assumptions but also for the difference of their averaging kernels. This work further shows that even when averaging kernels are considered in the comparison of two measurements, retrieval a priori influences from the assumed covariance matrix can still significantly affect the comparison. It is impractical to ask that all instruments retrieving a given quantity use the same a priori assumptions. However, for validation and intercomparison studies of the kind presented here it is nevertheless important that a common a priori be used to quantify the impact that this has on the apparent agreement (or disagreement) between two measurements. This will be particularly important in the production of climate-quality long-term data records that use sequential measurements from different instruments, for example, when extending the CO record from the current EOS sensors with that from the MetOp-A/Infrared Atmospheric Sounding Interferometer [*Turquety et al.*, 2004].

[43] **Acknowledgments.** This research was primarily sponsored by the NASA grant of the Aura Validation Project NNX07AB52G. D.P.E. acknowledges NASA support under grant NNX07AL57G. We would like to acknowledge the contributions to this work from other members of the MOPITT algorithm team at NCAR. Comments from Merritt Deeter and Rashid Khosravi from the Atmospheric Chemistry Division of the National Center for Atmospheric Research are also appreciated. The National Center for Atmospheric Research is sponsored by the National Science Foundation.

References

Beer, R. (2006), TES on the Aura mission: Scientific objectives, measurements and analysis overview, *IEEE Trans. Geosci. Remote Sens.*, *44*, 1102–1105, doi:10.1109/TGRS.2005.863716.

Beer, R., T. A. Glavich, and D. M. Rider (2001), Tropospheric emission spectrometer for the Earth Observing System's Aura satellite, *Appl. Opt.*, *40*, 2356–2367, doi:10.1364/AO.40.002356.

Bowman, K. B., et al. (2006), Tropospheric Emission Spectrometer: Retrieval method and error analysis, *IEEE Trans. Geosci. Remote Sens.*, *44*, 1297–1307, doi:10.1109/TGRS.2006.871234.

Deeter, M. N., et al. (2003), Operational carbon monoxide retrieval algorithm and selected results for the MOPITT instrument, *J. Geophys. Res.*, *108*(D14), 4399, doi:10.1029/2002JD003186.

Deeter, M. N., D. P. Edwards, and J. C. Gille (2007a), Retrievals of carbon monoxide profiles from MOPITT observations using lognormal a priori statistics, *J. Geophys. Res.*, *112*, D11311, doi:10.1029/2006JD007999.

Deeter, M. N., D. P. Edwards, J. C. Gille, and J. R. Drummond (2007b), Sensitivity of MOPITT observations to carbon monoxide in the lower troposphere, *J. Geophys. Res.*, *112*, D24306, doi:10.1029/2007JD008929.

Edwards, D. P., et al. (2004), Observations of carbon monoxide and aerosol from the Terra satellite: Northern Hemisphere variability, *J. Geophys. Res.*, *109*, D24202, doi:10.1029/2004JD004727.

Edwards, D. P., et al. (2006), Satellite-observed pollution from Southern Hemisphere biomass burning, *J. Geophys. Res.*, *111*, D14312, doi:10.1029/2005JD006655.

Emmons, L. K., et al. (2004), Validation of Measurements of Pollution in the Troposphere (MOPITT) CO retrievals with aircraft in situ profiles, *J. Geophys. Res.*, *109*, D03309, doi:10.1029/2003JD004101.

Emmons, L. K., G. G. Pfister, D. P. Edwards, J. C. Gille, G. Sachse, D. Blake, S. Wofsy, C. Gerbig, D. Matross, and P. Nedelec (2007), MOPITT validation exercises during Summer 2004 fields campaigns over North America, *J. Geophys. Res.*, *112*, D12S02, doi:10.1029/2006JD007833.

Ho, S.-P., J. C. Gille, D. P. Edwards, M. N. Deeter, J. Warner, G. L. Francis, and D. Ziskin (2002), Retrieval of surface skin temperature from MOPITT measurements: Validation and impacts to the retrievals of tropospheric carbon monoxide profiles, in *2002 IEEE International Geoscience and Remote Sensing Symposium*, vol. 6, pp. 3177–3179, doi:10.1109/IGARSS.2002.1027122, IEEE Press, New York.

Ho, S.-P., D. P. Edwards, J. C. Gille, J. Chen, D. Ziskin, M. N. Deeter, and G. L. Francis (2005), Estimates of the global 4.7 μm surface emissivity from MOPITT measurements and their impacts on the retrieval of tropospheric carbon monoxide profiles, *J. Geophys. Res.*, *110*, D21308, doi:10.1029/2005JD005946.

Kinnison, D. E., et al. (2007), Sensitivity of chemical tracers to meteorological parameters in the MOZART-3 chemical transport model, *J. Geophys. Res.*, *112*, D20302, doi:10.1029/2006JD007879.

Kulawik, S. S., et al. (2006a), TES atmospheric profile retrieval characterization: An orbit of simulated observations, *IEEE Trans. Geosci. Remote Sens.*, *44*, 1324–1333, doi:10.1109/TGRS.2006.871207.

Kulawik, S. S., J. Worden, A. Eldering, K. Bowman, M. Gunson, G. B. Osterman, L. Zhang, S. Clough, M. W. Shephard, and R. Beer (2006b), Implementation of cloud retrievals for Tropospheric Emission Spectrometer (TES) atmospheric retrievals: Part 1. Description and characterization of errors on trace gas retrievals, *J. Geophys. Res.*, *111*, D24204, doi:10.1029/2005JD006733.

Kulawik, S. S., G. Osterman, D. B. A. Jones, and K. W. Bowman (2006c), Calculation of altitude-dependent Tikhonov constraints for TES nadir retrievals, *IEEE Trans. Geosci. Remote Sens.*, *44*, 1334–1342, doi:10.1109/TGRS.2006.871206.

Lopez, J. P., M. Luo, L. E. Christensen, M. Loewenstein, H. Jost, C. R. Webster, and G. Osterman (2008), TES carbon monoxide validation during two AVE campaigns using the Argus and ALIAS instruments on NASA's WB-57F, *J. Geophys. Res.*, *113*, D16S47, doi:10.1029/2007JD008811.

Luo, M., et al. (2007a), Comparison of carbon monoxide measurements by TES and MOPITT: The influence of a priori data and instrument characteristics on nadir atmospheric species retrievals, *J. Geophys. Res.*, *112*, D09303, doi:10.1029/2006JD007663.

Luo, M., et al. (2007b), TES carbon monoxide validation with DACOM aircraft measurements during INTEX-B 2006, *J. Geophys. Res.*, *112*, D24S48, doi:10.1029/2007JD008803.

Olivier, J., A. Bouwman, J. Berdowski, J. Bloos, A. Visschedijk, C. van der Mass, and P. Zandveld (1999), Sectoral emission inventories of greenhouse gases for 1990 on a per country basis as well as on 1° × 1°, *Environ. Sci. Policy*, *2*, 241–263, doi:10.1016/S1462-9011(99)00027-1.

Pan, L., J. C. Gille, D. P. Edwards, P. L. Bailey, and C. D. Rodgers (1998), Retrieval of tropospheric carbon monoxide for the MOPITT Experiment, *J. Geophys. Res.*, *103*, 32,277–32,290, doi:10.1029/98JD01828.

Rinsland, C. P., et al. (2006), Nadir measurements of carbon monoxide distributions by the Tropospheric Emission Spectrometer instrument onboard the Aura Spacecraft: Overview of analysis approach and examples of initial results, *Geophys. Res. Lett.*, *33*, L22806, doi:10.1029/2006GL027000.

Rodgers, C. D. (1976), Retrieval of atmospheric temperature and composition from remote measurements of thermal radiation, *Rev. Geophys.*, *14*, 609–624, doi:10.1029/RG014i004p00609.

Rodgers, C. D. (2000), *Inverse Methods for Atmospheric Sounding: Theory and Practice*, World Sci., Singapore.

Rodgers, C. D., and B. J. Connor (2003), Intercomparison of remote sounding instruments, *J. Geophys. Res.*, *108*(D3), 4116, doi:10.1029/2002JD002299.

Tolton, B. T., and J. R. Drummond (1997), Characterization of the length-modulated radiometer, *Appl. Opt.*, *36*, 5409–5419, doi:10.1364/AO.36.005409.

Turquety, S., J. Hadji-Lazaro, C. Clerbaux, D. A. Hauglustaine, S. A. Clough, V. Cassé, P. Schlüssel, and G. Mégie (2004), Operational trace gas retrieval algorithm for the Infrared Atmospheric Sounding Interferometer, *J. Geophys. Res.*, *109*, D21301, doi:10.1029/2004JD004821.

Worden, J., S. S. Kulawik, M. W. Shephard, S. A. Clough, H. Worden, K. Bowman, and A. Goldman (2004), Predicted errors of tropospheric emission spectrometer nadir retrievals from spectral window selection, *J. Geophys. Res.*, *109*, D09308, doi:10.1029/2004JD004522.

D. P. Edwards, J. C. Gille, S.-P. Ho, and H. Worden, Atmospheric Chemistry Division, National Center for Atmospheric Research, PO Box 3000, Boulder, CO 80307-3000, USA. (spho@ucar.edu)

S. S. Kulawik, M. Luo, and G. B. Osterman, Jet Propulsion Laboratory, California Institute of Technology, 4800 Oak Grove Dr., Pasadena, CA 91109, USA.